

A Proposed Spacecraft Propulsion System*

*A design developed by Team 10 - Saturn V

1st Angel Alain Sosa Rodríguez
Technical University of Munich
Munich, Germany
angel.sosa-rodriguez@tum.de

2nd Aníbal Guerrero Hernández
Technical University of Munich
Munich, Germany
anibal.guerrero@tum.de

3rd Christian Racke
Technical University of Munich
Munich, Germany
christian.racke@tum.de

4th Ignacio Zúñiga Martínez
Technical University of Munich
Munich, Germany
i.zuniga@tum.de

Abstract—This document presents the design and analysis of a new spacecraft propulsion system for a mission to Phobos, one of the moons of Mars. The proposed propulsion system is based on a combination of chemical propulsion, utilizing liquid oxygen and methane as propellants. The mission analysis focuses on optimizing the trajectory and delta-v budget for the spacecraft, while ensuring that the spacecraft is able to achieve its scientific objectives while minimizing the mission cost. The results of the analysis show that the proposed propulsion system is able to achieve the required delta-v budget while also minimizing the overall propellant usage and power requirements. The paper also discusses various element configurations and technologies that were considered during the design process, and provides recommendations for future improvements on the system. Overall, the proposed propulsion system represents an alternative and new approach for deep space missions.

Index Terms—Spacecraft, Propulsion System, Phobos, GMAT, MATLAB, Pressure-fed, ACS, Hydrazine, MON-3

I. INTRODUCTION

The success of any deep space mission relies heavily on the propulsion system's ability to propel the spacecraft through space, achieve the required speeds and maneuver the spacecraft to its destination. The propulsion system is, therefore, a critical element in any mission, and the development and/or integration of new technologies plays an important role in reaching further distances in the vast universe. In this document, a proposed spacecraft propulsion system is being introduced for achieving the study of Phobos for 2 years. The proposed propulsion system is designed based on the mission analysis which derives the extensive development of the trajectory sequence and achieves the ΔV budget, mass budget, power budget. It aims to be efficient, reliable, and capable to successfully operate until the end of the mission, incorporating several key elements such as ACS reaction wheels, ACS Thruster, main thrusters and tanks as the proper technology needs. The study of the proposed spacecraft propulsion system presents the behavior and evolution of key parameters such as pressure and temperature, as well as the detailed configuration of the propulsion system.

II. WORK LOGIC, METHODOLOGY, APPROACH, PROCESSES

A. Working logic and methodology

The proposed spacecraft propulsion system was developed by conducting a mission analysis that aimed to send a satellite to Mars between 2026 and 2029. As an initial stage, extensive research about similar successful missions, conceptual definition of key parameters, as well as technologies implemented was performed with the objective of finding an optimal approach for the design stage. Subsequently, an iterative process to look for the best-fitted final results for a ΔV budget, propulsion system elements, configuration and schematic, and key parameter's behavior such as pressure and temperature, among others was developed. Finally, validation and re-calculation of the results within the given requirements and additional constraints are implemented. Throughout the extent of this document, the methodology remains similar in principle but aims to satisfy the special need of every case of study independently.

III. TOOLS

A. GMAT

One of the tools used for the trajectory and mission sequence alongside the development of the presented spacecraft propulsion system is GMAT. It offers accuracy in the trajectory design and calculation of the ΔV [1], being these the main reasons for its selection as a tool. This section aims to explain concisely the script, logic, and resources used within the software to calculate the trajectory and mission sequence. Likewise, a detailed explanation of the technical reasons behind these calculations can be found in subsection IV-B, as well as in subsection IV-C a theoretical approach is taken to explain the ΔV budget.

Main script: The initial conditions and parameters, such as C3 Energy and launching date, for the main script on GMAT are provided by the *Interplanetary Mission Design*

Handbook: Earth-to-Mars Mission Opportunities 2026 to 2045[2]. The script uses a *NewtonRaphson* algorithm with a *ForwardDifference* derivative method as a solver with a perturbation of 0.0001 aiming for an increase of results accuracy. A MJ2000Eq and MJ2000Ec coordinate system has been set for Earth, Moon, Mars, Sun, and Phobos. LEO, NearLuna Deespace, NearEarth, NearMars have been created as propagators with its central body described by their respective name or proximity. There are 7 principal impulsive burns and a corrective maneuver burn to maintain the phasing with Phobos. They have been created with the variable *origin* in function of its proximity to an astral body and/or location. Finally, as part of the initial settings, the spacecraft (called UXMAL on GMAT) works with an *UTCGregorian* epoch format and *OutgoingAsymtote* as its state type. A general approach can be seen in Figure 1.

1. *C3Burn*: This *Target* function calculates the necessary ΔV to achieve an Earth C3 energy of $9.144 \text{ km}^2/\text{sec}^2$. An impulsive burn named *C3Burn* is used, with origin in Earth, followed by a propagation of 1 hour, taking Earth as a central body. A *maneuver* function is used to calculate the necessary ΔV for achieving the requested C3 Energy.

2. *B-plane*: This *Target* function named *B-Plane* employs maneuvers in the Earth-based Velocity (V), Normal (N) and Bi-normal (B) directions by an impulsive burn named *TCM* (Trajectory Correction Maneuver) where the necessary ΔV is calculated for the elements *TCM.V*, *TCM.N* and *TCM.B* respectively. It includes four propagation sequences, taking Earth as a central body. The purpose of the maneuvers in VNB directions is to target *BdotT* and *BdotR* components of the B-vector. The proper calculation must achieve a value of *BdotT* targeted to 6800 and *BdotR* targeted to -700.

3. *MarsCapture*: This *Target* executes a maneuver with an impulsive burn named *MOI* which stands for Mars Orbit Insertion, it calculates the necessary ΔV to achieve a Mars RMAG of 100,000. This value represents the magnitude of the orbital position vector expressed in the MARS coordinate system[3]. A propagator to Mars Apoapsis is set within the *Target* function to model the motion just calculated, as well as a propagator for reaching a latitude of 0 with respect to Mars. All propagators within this function use a *NearMars* configuration.

4. *Inclination*: This *Target* function named *Inclination* fixes the angle of inclination of the spacecraft when entering Mars orbit. Through a maneuver executed by an impulsive burn called *INCB* (Inclination Burn), the necessary ΔV is calculated for the elements *INCB.V*, *INCB.N* and *INCB.B*. The function have the goal of achieving an angle of inclination of 0 degrees and a Mars RMAG value of 9389, which will serve the purpose of being in Phobos orbit.

5. *PhasingOrbit*: This *Target* function works coordinated with the following one *Circularorbit*. For instance, it has the goal to phase Phobos, since it is the goal of the mission to analyze this natural satellite of Mars. To do this, a series of iterative proof and error trials have been performed to find the adequate RMAG value (For this case it is calculated RMAG equal to 22325), and the estimation was mainly visually based. Once the required position has been achieved, a maneuver is used to obtain the spent ΔV . The maneuver is carried out by an impulsive burn named *PPB* (Phobos Phasing Burn). Then, it propagates for 1 day and to Mars periapsis using a *NearMars* propagator.

6. *CircularOrbit*: This *Target* function finishes the task created by the previous one, *PhasingOrbit*. To fully achieve the phasing of the spacecraft with Phobos, it is necessary to fix the spacecraft's orbit, from an elliptical one to a circular one. For this, another maneuver by an impulsive burn named *POI* (Phobos Orbit Insertion) is employed to achieve a value of RMAG equal to 9389 which will be propagated to Mars Apoapsis by a *NearMars* propagator.

7. *CorrectiveBurn*: This *Target* function calculates the necessary ΔV for keeping phase with Phobos, for this an impulsive Burn named *CBP* (Corrective Burn Phobos) is used. Where a value of RMAG equal to, 9500 is achieved. As this is a burn that will be executed many times during the spacecraft's operative life, it has been decided to treat it as a series of periodic burns making a conceptual separation from the other 7 main burns, but including its ΔV cost in the calculation and design of the system just as the other burns. On subsection IV-B can be found the approach to the periodicity previously mentioned.

8. *Deorbitting*: Finally, this *Target* function aims to reduce the distance between the spacecraft and Mars. At the end of the mission, a deorbiting maneuver will be performed. Using the impulsive burn named *DEO* (De orbiting), the function calculates the necessary ΔV to achieve a value of Mars RMAG equal to 5400 for deorbiting the spacecraft.

B. MATLAB

To facilitate the quantitative comparison of different concepts and the automation of calculation loops, a MATLAB script was set up. It implements the computation and verification of all the relevant design values involving the spacecraft's mass, propellant, and power budgets as well as the thermodynamic states in both the helium pressurization gas tank and the propellant tanks. The following section deals with the explanation of said MATLAB script. Here, its main working logic and the flow processes it goes through are presented and analyzed. This section however does not give thorough explanations or justifications on the physical phenomena implemented, all of this will be covered with

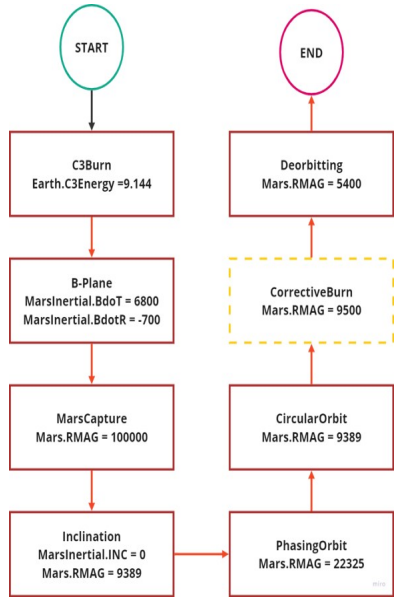


Fig. 1: Mission sequence

greater detail in section V.

Principally, the MATLAB code basis created for the project includes one main script (its flowchart is represented in Figure 2 for reference) and many functions. This division helps keep the code clear and understandable, which also aids its compatibility with and transferability to other projects in the future.

Main script: The main script starts with the initialization of all the important input parameters, out of which the most notable ones are (all in SI units): ΔV for each maneuver in a vector, engine parameters such as ISP and mass flow, tank pressures and temperatures as well as dry masses of different components that can be predetermined. It then goes through three main calculation loops, with the principal one providing a first estimation of the overall system mass including the tank masses and volumes for both the propellant tanks as well as the helium pressurization gas tank. For this, it mainly calls three functions, namely *spacecraft_mass_iter*, *volume_sizing* and *tank_dry_mass*. Short descriptions of the respective functions themselves can be found below.

Eventually, the loop is exited on the condition of convergence, meaning that the dry mass of the spacecraft has not changed significantly from one loop to another (the margin for that can also be changed at the beginning of the script). The second loop handles the numerical pressure depletion and subsequent initial volume adaption of the helium tank. This is mainly done by calling the *dynamic_tank_sizing* function for each maneuver (with a temperature reset and partial pressure reset resulting from it in-between), which calculates the temperature and pressure evolution over time in the helium tank. It is then checked if the pressure in the said tank has

dropped below the minimum acceptable pressure and - if not - the starting volume for the calculation is lowered slightly. The numerical computations are then repeated until the pressure minimum in the tank coincides with the acceptable minimal pressure at the regulating valve [4]. On top of that, the behavior of the gas when passing the regulating valve and after it has entered the respective propellant tank is computed as well. The script then turns to the last and usually smallest loop. Here it does the final mass calculations for the tanks' masses, volumes, and the overall spacecraft mass by once again calling *spacecraft_mass_iter* and *tank_dry_mass*, now with the readjusted helium tank volume fixed. Once more, the loop is being exited under the condition of convergence of the spacecraft's dry mass. To finish, the script outputs the relevant values in a table and plots the temperature and pressure depletion in the pressurization and propellant tanks over time. Finally, two more comments are required: First of all, the script repeatedly checks if critical thermodynamic points of any of the fluids are reached/passed (this will be discussed in section V) and if the script is converging within the set limits. Should any such point be reached or the convergence is not fulfilled, it will be displayed in the last column of the output table checking for validity. Secondly, a larger version of this code exists, which includes loops for different engines/pressurization gas combinations. This slightly larger script was meant to aid the decision-making for the type of pressurization gas and engine combination but was later (after that decision had been made) abandoned for computational efficiency reasons (the calculations for the numerical pressure/temperature depletion can take quite a long time when choosing a reasonably small step time). It can however be easily adapted and utilized for future design trade-off analyses. The most important takeaway from these comparisons was that helium, even though it is more expensive, has proven to be the pressurization gas of choice due to the significant wet mass savings that have shown to be associated with it (in comparison to using Nitrogen).

Function spacecraft_mass_iter: This function provides the calculations for the resulting wet masses based on the Tsiolkovsky rocket equation [5]. Since (and under the assumptions made for this project) the total dry mass depends both on itself (since dry mass effects harness mass) as well as on final wet mass (which affects structural mass), a loop was implemented to compute the final wet mass as a repetitive process.

Function volume_sizing: This function gives a first estimate of the pressurisation tank volume based on the propellants tank volumes and pressures as well as thermodynamic correlations for the ideal gas (which can be found in [6]).

Function tank_dry_mass: This function calculates the dimensions and masses of the gas and propellant tanks according to Barlow's formula [6].

Function dynamic_tank_sizing: This function implements the thermodynamic approach presented in [7] to numerically calculate the pressure and temperature depletion in the pressurization tanks. It also calculates the thermodynamic state of the gas when reaching the respective propellant tank (i.e. after the regulating valve). To achieve this accurately, the *CoolProp* library is utilised to retrieve the relevant thermodynamic properties at different states of the fluids.

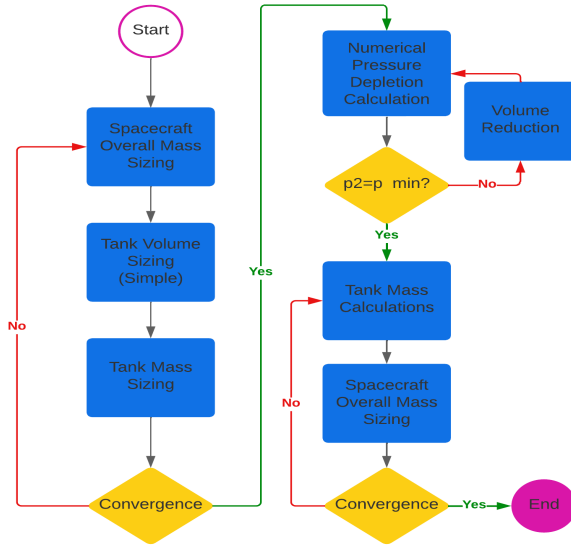


Fig. 2: MATLAB main script flowchart

C. Trade-off Analysis

The trade-off methodology followed in the project consist on:

- First, define the most relevant parameters which can define the performance and success of the elements or system that need to be compared.
- Second, all the parameters are compared between them, setting a value of 1 if the parameter is less important than the compared one, 2 if the parameters are equally important, or 3 if the parameter is more important.
- Once defined the parameter's relevance, all the parameter scores are summed up and divided by the total number of points, obtaining a decimal weight of the parameters.
- For each option, a score of the different parameters is set. Being the higher the best. The range of the score could vary, but in most cases is between [1,5], with 5 being the best score and 1 the worst.
- Finally, the candidate's parameters scores are multiplied by the weight of each parameter and summed up obtaining a final score for each option.

IV. MISSION ANALYSIS AND OVERALL SPACECRAFT

A. Assumptions, trade-offs and their justifications and impact

Following the ECSS standards [8] [9] a trade-off analysis has been performed for selecting the propellant type and composition. From the parameters stated in the standards, some sub-parameters have been defined:

- *Isp*: The specific impulse of the propellant is a measure of the propulsion efficiency and is directly related to the propellant mass.
- Thrust: Certain maneuvers (Hohmann) require enough level of thrust. Furthermore, it influences the safety of the mission and relates to the mission time.
- Mission time: Long exposure to space radiation can affect the hardware functionality. As the sensibility of the equipment to radiation is not stated, mission time has been considered a key factor to achieve mission success.
- Propulsion system restart: Compares the possibility to re-start the engine and the ease to do so. According to the requirements, the propulsion system must be able to restart.
- System complexity: The complexity of the propulsion system affects negatively the probability of success.
- Total system mass & volume: Compare the total mass and the volume of the system, as some types of propulsion hardware mass and volume differ notably from others (Nuclear, Solar Sails).
- Required power: Some types of propulsion systems require a high amount of power, being necessary to include the means to provide it. Other systems' power requirements are not included.
- System compatibility: Electromagnetic interference can affect communications with the spacecraft. The EMC of the propulsion system with the rest of the systems of the satellite must be ensured.
- Contamination: Compares the overall contamination produced by the system and the operator's risk during the manufacturing of the spacecraft.
- Technology Status: Experience is a key factor in leading to success. Compares the development level of the technology based on the TRL [10].
- Availability: Compares the market availability of the different components of the propulsion system.
- Total cost: Even if the system's performance & success have been optimized, the cost is still a leading factor in the design of every engineering system. Overall system cost including components and propellant has been taken into account.

It can be observed that some parameters may have some type of correlation to others, for example, thrust and mission time. Nevertheless, none of the parameters can be fully encapsulated in another one, as for example Thrust, also affects other aspects such as maneuverability and safety (emergency course corrections). Even so, 'bigger' parameters such as mission time, total mass, or cost have always been evaluated as more important when compared to 'smaller'

ones. In other words, the 'bigger' parameters are divided into smaller ones, that also take slight differences into account. This parameter selection has been designed to have a deeper analysis of the options and not only focus on these main parameters. Following the methodology stated in subsection III-C the weighting of the values is performed Table XIV.

Once the parameters are defined, a numerical or qualitative value has been fixed for each option's parameter. Ending up with the resulting layout Table XV. The data has been collected from different sources divided into Lecture Material [4] [6], suppliers datasheets [11] [12] [13], and webs [14] [15].

Multiplying each value times the respective weight, we can finally obtain the scores Table XVI. Even though the electrostatic and the liquid propellant have close scores, the liquid bi-propellant has been selected as the propellant type. The combination of a high thrust which helps to have high maneuverability and achieve short burning times, is the most suitable for the mission requirements, maintaining a satisfactory level of cost and mass budget, and the well-establishment of the technology, makes it the strongest option for the mission.

B. Trajectory and Mission Sequence

One of the main stages of the development of the propulsion system is the trajectory and mission sequence. These aspects construct the backbone of key parameters such as the mass budget and let alone predict and detect temperature and pressure behaviors. Consequently, aid from the GMAT system has been implemented since it is desired to achieve as much accuracy as possible (See subsection III-A). Nevertheless, it is important to mention the *physical* phenomena of this trajectory and mission sequence. The first approximation was based on the Deimos mission by NASA [16], where it served as an initial point for clearing questions about which techniques and technologies to use as well as reached achievements of that mission. Then, the launching windows of opportunities handbook developed by NASA [2] has been used to approach the case of study within the scope of the date requirement. As a robust theoretical approximation, it is also taken into account the use of a Hohmann-Transfer with the amount of C3 energy stated in the NASA handbook for escaping Earth. Hence, it is estimated to be launching between 2026 and 2029, 3 different dates are chosen to be evaluated: 2 dates in the year 2026 and 1 date in the year 2028. As follows, After a previous analysis of the mission requirements and goals, it was decided to launch the spacecraft on the 31st of October 2026 (See subsection IV-C). The C3 energy needed at this date is considered of $9.144 \text{ km}^2/\text{s}^2$ and the launch site is meant to be the Guiana Space Center due to its location and long history of successful deep space mission [17][18][19]. Following, it is shown the trajectory and mission sequence, shown by its 7 main burns and its corrective burns, from a theoretical point of view where it is

intended to apply the concepts and techniques gathered from the sources of information previously mentioned.

The mission sequence consists of the following burns:

- C3 Energy: In order to escape Earth's gravity and be able to set the spacecraft in direction to the following maneuvers and Phobos itself, it is necessary to reach a Characteristic Energy or C3 of $9.144 \text{ km}^2/\text{s}^2$ [2].
- B-plane: Once Earth's gravity has been overcome, the spacecraft is able to start its journey to Mars and eventually Phobos. To do this, Mar's B-plane is targeted[20] which thanks to a gravity assist can put the spacecraft closer to Mars. A total of 295 days has been spent in this maneuver, however, the time consumed profits with a cheap ΔV budget cost.
- Mars Capture: Once the spacecraft is closer to Mars, another maneuver is to be performed with the objective of inserting itself in the martian orbit. It achieves an elliptical orbit that later must be corrected to meet Phobos's circular orbit. This closes the B-plane targeting of Mars.
- Inclination: When finishing the B-plane targeting, the spacecraft inserts in Mars orbit with a degree of inclination. It is now necessary to correct this inclination in reference to the inertial body of Mars. An amount of ΔV is spent in reaching a 0 degree of inclination as well as positioning the spacecraft at the same distance that Phobos with respect to Mars (9389 km).
- Phasing Orbit: It is now necessary to phase Phobos to fulfill the mission goals of studying this natural satellite for 2 years. To do that, it is aimed to perform a burn that provides the necessary distance within the spacecraft orbit to match Phobos and thus achieve the phasing. Nevertheless, it is also necessary to perform a subsequent maneuver so that once the phasing has been reached, the orbit with Phobos could be maintained. For doing so, another maneuver would be necessary.
- Circular Orbit: To finally achieve the complete phasing process, a burn fixes the spacecraft's orbit from an elliptical one to a circular one. It is aimed to have the same distance of apoapsis and periapsis, taking Mars as the point of reference.
- Corrective orbit: Once the spacecraft is phasing Phobos, due to the orbital period of approximately 8 hours (7 hours and 39 minutes) of Phobos, it will be necessary to perform periodical burns to correct the phasing. For this, a series of burns are to be executed approximately every 20 days to fix the position of the spacecraft. This period of time has been set to take into consideration the total duration of 2 years mission, which at the end will result in a total of 36 corrective burns. However, all of them are integrated into the total ΔV budget. The execution of this maneuver, in contrast with the rest of the burns, is performed by the main engine, ACS reaction wheels, and ACS thrusters, executing this periodic maneuver as explained in subsection V-I.

- De-orbiting: Finally, at the end of the mission, the spacecraft will be de-orbited to the martian atmosphere by reducing its altitude with respect to the periapsis. This is the last amount of ΔV spend and thus the end of life for the spacecraft.

C. Delta V Budget

In subsection III-A and subsection IV-B the trajectory and mission sequence have been already analyzed from two different perspectives. The methodology, assumptions, and processes for the calculation of the necessary ΔV have also been stated there. However, it is optimal to display the final process towards the selection of the ΔV used for the presented propulsion system. Since the mission itself is estimated to be launched between the years 2026 - 2028, a trade-off of the different ΔV Budget per launching date has been performed with the purpose of finding the most suitable one, or the less costly. As it can be seen in Table I there are 3 dates taken into the analysis: 2 dates in 2026 (31/10 and 14/11) and one date in 2028 (12/10). These values are calculated by keeping the approach of the mission and trajectory sequence but modifying the launching date of the script in GMAT, the C3 energy, and the variable values if needed. Finally, from this trade-off, the best ΔV budget has resulted to be the one from the launching date on 31st of October 2026, as it can be seen in Table II. Likewise, the Table I displays the ΔV budget trade-off as a function of the launching dates already mentioned.

TABLE I: ΔV Budget Trade-off

-	-	31/10/2026	14/11/2026	12/10/2028
No.	Maneuver	ΔV [km/s]	ΔV [km/s]	ΔV [km/s]
1	C3Energy	0.23118	0.38307	0.22370
2	B-Plane	0.56795	0.55055	1.11494
3	MarsCapture	0.88005	1.06595	1.99732
4	Inclination	0.31958	0.12090	0.22506
5	PhasingOrbit	0.32491	0.35278	0.35058
6	CircularOrbit	0.3982	0.39851	0.39834
7	CorrectiveBurn	0.00626*36	0.00647*36	0.00632*36
8	Deorbiting	0.30977	0.82788	0.30976
	Total	3.25741	3.93264	4.84750

TABLE II: Final DV Budget

-	-	31/10/2026
No.	Maneuver	ΔV [km/s]
1	C3Energy	0.23118
2	B-Plane	0.56795
3	MarsCapture	0.88005
4	Inclination	0.31958
5	PhasingOrbit	0.32491
6	CircularOrbit	0.39826
7	CorrectiveBurn	0.00626*36
8	Deorbiting	0.30977
	Total	3.25741

V. PROPULSION SYSTEM

A. Propulsion System Requirements

According to the previous ΔV and other general requirements and the propulsion system must meet the following requirements:

- Provide the seven impulses, being capable to restart and pause the engine within the required time.
- Provide enough thrust to be able to follow approximately the ideal orbit transfer.
- The propulsion system must have the capability to control the attitude of the satellite.
- Thrust must be sufficient for approximate ideal orbit transfer.
- Correction maneuver must be obtained with the attitude control system.

B. Assumptions, trade-offs and their justification and impact

Once defined the propulsion type, another trade-off has been performed to select the exact type of propellant and thruster. As this decision is heavily influenced by the market availability, instead of comparing the propellants first, a comparison of the main engines has been directly carried out, comparing engine performances even though they use different types of propellants. Consequently, the analysis can specifically point out an engine if the performance is good enough without filtering or pre-selecting one type of propellant, without leaving out possible candidates from the comparison. This way, the main bi-propellant engines and their characteristics from *Ariane Space* [13], *Aerojet Rocketdyne* [11], *Nammo* [21] and *IHI Aerospace* [22] have been compiled in Table XVIII.

From this wide variety of characteristics, the most important ones have been filtered and selected. Again, the criteria for selecting the parameters was based on the ECSS standards [8]. Apart from some of the previous parameters, two new parameters were included:

- Pressure inlet: Value the reduction of the pressure inlet while keeping the nominal performance. A low-pressure inlet is beneficial for the pressurant and tank masses.
- European supplier: Maintaining the ESA approach, European engines have received a bonus.

Performing an analogous process as the one stated in the subsection III-C, the weight of each parameter can be computed Table XVII. However, as observed in Table XVIII, the engine parameters are quite similar. For this reason, a normalization between one and ten has been performed. This way the scores are widened and the analysis can be improved. Aligned with the rest of the project, the performance and mission success has been the priority over the selection of the parameters. It is important to notice, that as the performance is quite similar, the price of the engine could have been a determinant factor in the selection of the engine, unfortunately, companies are quite opaque with prices. For this reason, a boost in the weight of the propellant cost, trying to compensate for the poor information about engine prices. As propellant prices are also sensitive to market and suppliers, the *DLA Standard Prices for Aerospace Energy* [23] has been used as a reference.

Finally, the scores of the different engine options can be obtained in Table XIX. Several conclusions can be obtained from the analysis. Overall, hydrazine engines have better performance values than MMH engines, and European engines' low *ISP* keep them out of the top. Apart from these conclusions, two engines point out. The first one is the *AMBR 556N Dual Mode High Performance Rocket Engine* from *Aerojet* and the second one is the *Hydrazine Thruster* from *IHI*. Both engines use hydrazine and MON-3 as propellants and are excellent in the performance section, archiving the best value of the *ISP*. The main difference between them is the Thrust, being superior in the *AMBR*. As explained previously, this increment of thrust can be beneficial to mission safety, apart from reducing the mission time. However, the other important difference is that the *AMBR* is not fully qualified for flight, while the *IHI* engine is completely qualified and market available. Since the launch time is expected to be 2026, and a rough estimation of the flight qualification process is two years, given the slight superiority of parameters of *AMBR*, it has been chosen as the main engine. Nevertheless, the *IHI* engine is left as a second option in case it would not be possible to fully qualify the *AMBR* by the launch date.

C. Description of the propulsion system architecture and design decisions

Following, an overview of the proposed engine is shown. The details of the design and selection of the different components are presented in the next sections.

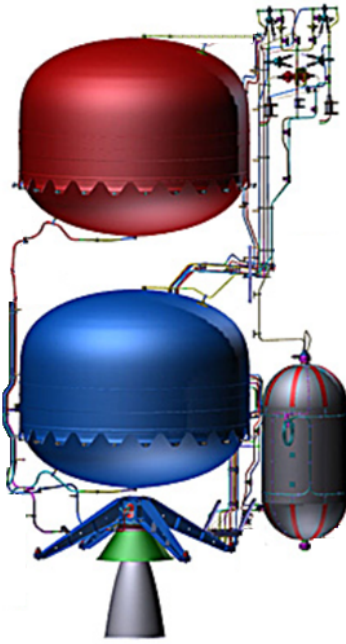


Fig. 3: Scheme of the selected architecture (Based on [24])

The presented liquid bi-propellant propulsion system is a pressure-fed engine that uses Helium to feed two tanks of hydrazine and NTO (MON-3). A two tanks cylindrical configuration has been selected over a four-tank design for

several reasons. The two tanks configuration, as it has half the propellants tanks, has fewer valves and pipes. This reduction in the components and complexity is traduced in a reduction of the failure probability of these elements, increasing the reliability of the mission, on which we have focused. This architecture is also beneficial as the main center of gravity shift is on the z-axis of the satellite. This is helpful to reduce the complexity of the attitude control system, orientate correctly the spacecraft and ease spacecraft operations.

The attitude control system selected is a 3-axis stabilized. The main attitude control operation would be carried on by a set of four reaction wheels, one for each axis and a redundant one. The system also counts four small bi-propellant thrusters for the desaturation of each reaction wheel and for emergency purposes.

D. P&ID / Schematic of the propulsion system

The system schematic diagram is illustrated in Figure 4. The engine system is made up of two big sections: the pressurant gas feed system and the propellant feed system.

The pressurant gas tanks are discussed in subsubsection V-I4. This material has good mechanical properties (high strength and resistance to fatigue) which make it ideal for high-pressure applications.

Fill and drain valves (FDV) are used to control the flow of fluids in the system by loading or venting the pressurant, propellants, and propellant vapor. These valves can be found all throughout the schematic, between every and each closed section. For example, FDV2 is a closed section between the pyrotechnic valves normally closed and the pressure regulator PR1.

pyrotechnic valves can be found in two states - normally closed and normally opened. When one activates, the valve irreversibly changes to its contrary state, meaning a normally opened valve will close when activated. pyrotechnic valves have several functions in this P&ID which will be explained progressively later.

Filters will protect sensitive components of the architecture, such as pressure regulators, check valves, and thrusters. Contaminants, particulate matter, or debris may affect readings that must be precise, stop valves from closing, or reduce combustion efficiency respectively.

Double-pressure regulators lower the high pressures in two stages. They provide a constant delivery pressure without the need for periodic readjustment, working exceptionally well for high-pressure cylinder applications, such as the pressurant gas tank. Pressure sensors translate the physical pressure exerted on the sensor as an output signal that can be used with a pressure regulator to control the pressure delivered.

The propellant tanks are later discussed in subsubsection V-I4.

Latch valves control the flow of the fluid with precision. When a latch valve is in its "off" position, it blocks the flow of fluid. They are ideal for remote applications as they have a low power consumption.

A more precise explanation of the schematic can be provided by following the mass flow:

Initially, pressurant gas is stored in the tanks. A pressure sensor (*PS1*) right beneath the tank will determine if the initial pressure at which the gas is liberated is adequate. The first set of pyrotechnic valves encountered is six pairs of antagonist valves working together - one normally open (*PVO*) and one normally closed (*PVC*), and an additional *PVC7* (total set from *PVO1* to *PVC7*). Due to the mission characterization, the minimum ΔV requirement was found when the trajectory was optimized to have seven separate impulses. For the first burn, *PVC1* will open at the beginning of it and *PVO1* will close at the end of it. This will occur for the rest of the burns, except for *PVC7*. As the last burn corresponds to the termination of the mission by crashing the spacecraft into Phobos, the depletion of the gas tank is desired to prevent explosions and reduce the velocity of the spacecraft as much as possible so that it can be captured by Phobos adequately, falling and crashing into its surface.

Then, a filter (*F1*) and a double pressure regulator (*PR1*) are placed in series. The filter will clean the gas before it enters the regulator, and will then be regulated to the pressure required for the propellant tanks. If *PR1* fails, *PVO7* will activate, closing that piping section and *PVC8* will open when activated, allowing the gas to flow through the other filter (*F2*) and regulator (*PR2*) placed in parallel. A posterior pressure sensor (*PS2*) is placed after the regulators to verify that the outputted pressure is correct.

Later, the gas encounters another filter (*F3*), and two check valves (*CV1*, *CV3*), placed in series to prevent backflow. The filter eliminates any contaminants, preventing blockage of check valves. However, the backflow of the propellant is dangerous and undesirable. Therefore, two check valves are used to accomplish this requirement, increasing safety and ensuring further the success of the mission. The two branches from here forward are identical and symmetrical. The left branch is followed as an example.

Historically, the propulsion system is the major cause of mission failure. Therefore, propellant flow to the thruster must be ensured through redundancy. For this reason, two pyrotechnic valves (*PVC9*, *PVC11*) are placed after the propellant tanks. They provide the first step towards redundancy. In case *PVC9* does not open upon activation, *PVC11* can act as a backup. Additionally, two pressure relief

valves (*PRV1*, *PRV2*) are placed to prevent the system from exploding due to overpressure. Using the two pressure sensors (*PS2*, *PS4*) before the propellant tanks, the relief valves will automatically open and release pressure preventing equipment damage.

Posterior, piping is split into two as there is a branch separation. Here, most of the propellant mass flow will be directed toward the main thruster. However, the rest of it will be utilized by the pair of attitude control thrusters (*ACT1*, *ACT2*). These two, smaller thrusters are part of the attitude control system. The attitude control system is composed of four reaction wheels and the *ACT1*, *ACT2*. These work due to the conservation of momentum. However, when a wheel has accumulated too much angular momentum, they are no longer able to provide the necessary torque to control the spacecraft's attitude. That is when the two smaller thrusters desaturate the reaction wheels by removing the excess angular momentum (further comments on the attitude control system are addressed later). Therefore, a filter is required before the mass flow reaches the attitude control thrusters. However, the filter *F4* is placed before the branch separation as both branches can separate from the filter. The filter is able to clean any contaminants that are carried by the mass flow stored in the propellant tanks. This may occur because the propellant may react with the tank walls due to minor incompatibilities for long periods of time stored until the end of the mission.

Following the main thruster branch, the second redundancy system is encountered. Initially, the mass flow would pass through *PVO8* and into the latch valve *LV1*. In case of failure of the latch valve, *PVO8* is closed and *PVC9* opens, allowing mass flow through *LV2*. Afterwards, a pressure sensor (*PS7*) controls proper input pressure to the main thruster, and a final filter (*F5*) cleans any possible debris, preventing losses in combustion efficiency. Like most commercially available thrusters, the thruster selected has integrated latch valves that serve as the third and final redundancy system. It is essential for the piping to be sufficiently safe but also optimized to reduce weight and ultimately costs of the mission.

Finally, by following the attitude control thruster branch a pressure sensor (*PS5*) reads the pressure, and the branch is divided again into four subsequent branches regulated by four latch valves (*LV5-8*), corresponding to each thruster (*ACT1-4*) respectively.

E. List of equipment

A list of all the relevant subcomponents used in the P&ID is listed in Table III

The unit mass of each subcomponent has been obtained from [25], [26].

F. Spacecraft Mass and Power Budget

The following subsection discusses the overall physical design of the spacecraft with a special emphasis on its

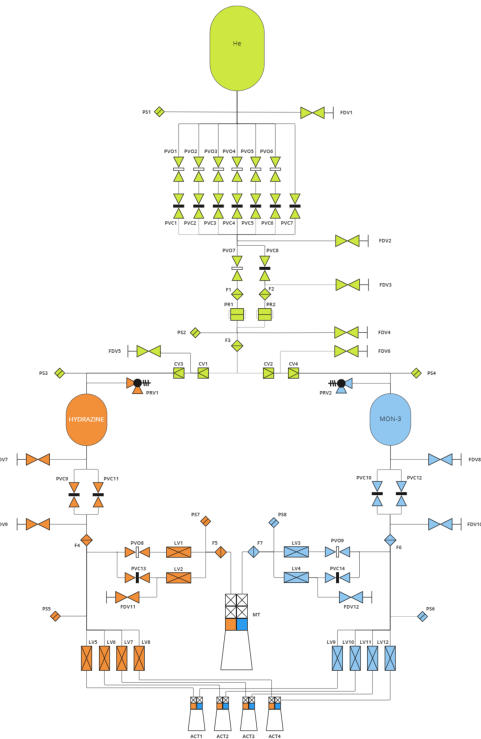


Fig. 4: P&ID schematic diagram of the propulsion system.

TABLE III: P&ID legend and list of equipment required.

Subcomponent	Acronym	Quantity	Unit Mass [kg]	Total Mass [kg]
Fill and Drain Valve	FDV	12	0.10	1.20
Pressure Sensor	PS	8	0.23	1.84
Pyrotechnic Valve - normally open	PVO	9	0.20	1.80
pyrotechnic Valve - normally closed	PVC	14	0.20	2.80
Filter	F	7	0.10	0.70
Pressure Regulator	PR	2	2.31	4.62
Check Valve	CV	4	1.36	5.44
Pressure Relief Valve	PRV	2	0.20	0.40
Latch Valve	LV	12	0.34	4.08
Main Thruster	MT	1	4.90	4.90
Attitude Control Thruster	ACT	4	0.97	3.68

propulsion system. This mainly refers to the calculation and presentation of results for the most important mass relations of the system such as wet and dry mass, but will also include a short paragraph about the most relevant ensuing volumetric dimensions as well as the assumed electrical power consumption. This part will mostly follow the same steps as were already presented in subsection III-B, but instead of focusing on the computational specifics, the spotlight here will be on the physical relations underlying these calculations as well as on the presentation and justification of the assumptions made during the process.

The most basic formula necessary for any such calculation is the Tsiolkovsky rocket equation [5]. As also for the assumed given relationships between the harness mass, electrical power, dry mass, and wet mass, this shall not be elaborated any further since no project-specific insights can be gained from it. The only point left to mention here is that since the required electrical power of the valve is not explicitly stated in Aerojet Rocketdyne's data sheet for the chosen engine, it was conservatively assumed to be 45 Watts (conservatively

because compared to other engines of the same manufacturer and where said value is stated, 45 Watts is on the upper end of the range and only required in engines with a higher thrust and mass flow [11]). The other two elements in Table VII are the assumed electrical power consumption of all other subsystems as required by the project demands and the electrical power for the attitude control system, which will be investigated more thoroughly in subsection V-I. The first point to talk about is the margins that apply here. As is standard for conceptual design phases, multiple such margins are implemented [27]. For this project, two main mass margins were added accordingly: The first being a 15% margin on the propellant required and on top of that a 20% overall system margin added on all of the designed masses. However, since the project's description only accounted for said system margin, an approach in accordance with ESA's margin philosophy was chosen [28]: The 15% extra propellant is accounted for in the tank sizing calculations (and therefore increases dry mass slightly by making the system "ready" to take the extra propellant), but it is not added to the required propellant itself in the end, which also ensures consistency with respect to the rocket equation and the relationships between wet mass, dry mass, and fuel mass. Overall, these margins lead to a significant increase in the projected spacecraft mass, thereby providing a reliable safety net in case unexpected design changes have to be made later in the development process. All of the margins mentioned in this section can be found summarised in Table IV. The respective values stated in the table are factors, meaning they have to be multiplied by the original values in order to get the result required.

The next relevant margins are related to the fill volumes. As stated in the project description, an ullage volume of 2% shall be taken into account for the propellant tanks' sizing calculations. For the helium pressurization tank, however, a 20% margin on the gas volume and mass (in accordance again with ESA regulations [27]) is applied. For the first estimation of said required volume, a simple ideal gas process was assumed with a polytropic exponent for the helium of $n=1.2$ (the value is usually between 1.1 - 1.2 for this type of application [6]). Since the actual volume is later refined in a more sophisticated analysis, this value and the specifics of that analysis only have a limited effect on the calculation results. As a reference value, the difference between $n=1.1$ and $n=1.2$ (compared to $n=1.15$ respectively) for the final wet mass has shown to be about 13kg. While this might seem like a lot at first sight, it turns out to be less than 4% of the added weight just due to the system margin. Nevertheless, $n=1.2$ provides the most conservative estimates in that regard and was therefore chosen.

Consequently, the estimation for the tank masses shall be explained now. For this calculation, Barlow's formula [6] was used to determine the minimum wall strength and subsequent minimal tank mass. This method however does

neither include possible safety margins nor does it account for the additional weight added by things such as bearings, instruments, etc. In order to get a realistic and reliable value for that, the results from the calculations of the script were compared to actual values in the tank catalog data sheet from the company MT Aerospace [29]. This was done with multiple operating pressures and tank concepts from the mentioned catalog. It leads to two different safety/realism margins; one for the helium tanks and one for the propellant tanks. The difference between 1.75 for the former and 2.5 for the latter can be explained by two things: First of all, they operate under substantially differing pressures, altering the general tank design concept to a significant degree. Secondly, and also due to the characteristic pressure ranges for each, they use different materials. While the propellant tanks in question use titanium alloys for the whole tank essentially, the high-pressure tanks in question use a mixture of titanium alloys for the shell and an overwrap of epoxy-based carbon fiber. Generally, the mentioned margins were calculated as a rounded average of different compared ratios between script and real values.

The most interesting part of the calculations certainly is the refining of the helium tank's volume and the accompanying control checks of possible thermodynamic phase changes. First of all, the estimate for the volume - as explained earlier - is taken as the starting point. Then, a numerical computation of the more exact behavior of the gas while expanding and cooling down in the tank, as well as its behavior while being passed through the throttling valve and into the propellants tanks is performed. For each (small) time step, first, the resulting pressure and temperature depletion in the tank are calculated. Then, the behavior at the throttling valve is investigated. At said valve, and when helium is viewed as a real gas rather than an ideal one, the helium experiences a temperature change opposite to what the ideal gas behavior might suggest: It heats up. This so-called Joule-Thomson effect is taken into account to calculate the temperature of the gas reaching the propellant tanks and is relevant for three ensuing checks: First, it has to be checked if the gas itself through that expansion and subsequent cooling (which can happen at the throttle valve for gases which experience the opposite Joules-Thomson effect such as nitrogen; the script was written so that it can handle other gases and their behavior as well) reaches temperatures below its own boiling point (reference value taken from [30] and would therefore liquefy. The second check regards possible phase changes in the propellants: Each for the NTO oxidizer (reference values taken from [31]) and for the hydrazine fuel (reference values taken from [32] and [33]) it is checked whether the temperature of the arriving helium gas is neither above the boiling point nor below the melting point. Here, the different maneuvers come into play. Due to the vast amount of time between each maneuver, it is considered that the gas in the propellant tanks assumes the temperature of those propellants. This means that for this second check (naturally only after

the first maneuver is completed), a mixture between the new incoming gas and already existing gas is taken into account and a mean temperature is calculated by considering the volume ratios between them. Lastly, and also due to the reheating of the gas in the propellant tanks, the pressure increase due to this temperature rise is calculated similarly on the basis of the temperature after the throttling valve (i.e. the temperature of the gas when reaching the propellant tanks). It is thereby verified that the maximum pressure does not exceed the operational pressure plus an already factored-in pressure margin which was accounted for as a result of previous iterations. This maximal pressure increase calculated has shown to be around 1.4 bar, with conservative rounding this becomes 2 bar. Since the chosen engine has an inlet pressure maximum of 11.7 bar, on top of which usual losses of 20% for the injection and 5% for the piping and valves are added [4], the required propellant tank pressure solely from that requirement is 14.625 bar (again conservatively rounded to 15 bar). The tanks, therefore, have to be certified for a maximal expected operating pressure of at least 17 (15+2) bar. This is therefore also the design pressure used for the tank calculations. Generally, these pressure rises are relatively low, which is partially also due to the large margins for the propellants and the resultant excessive volumes stored in the tank as well as the comparatively small maneuvers towards the end of the spacecraft's lifetime.

All things considered, the final values for the spacecraft's masses and volumes can be found in Table V and Table VI, respectively. Included in the stated mass for the propulsion system are - on top of the engine's mass - both the masses for the whole tank system as well as for the helium mass. The stated mass for the attitude control system consists of the masses of the reaction wheels/thrusters and the required propellant mass for such operations as well. This additional propellant is considered to be dry weight but was accounted for in the tank sizing. The most important point to take away here with regard to the feasibility of the design is that the projected final mass and volume - including all margins as stated above and also when adding the payload adapter mass of 85kg to the spacecraft's mass - are both within the maximal mass that the Ariane 62 is capable of sending on an earth escape trajectory (2600 kg [34]) as well as within the maximal volumetric capacities (14 or 20m height, 5.4m diameter [34]) of its fairing. Lastly, in Table VII the required power budget can be found as well. Details on where these values come from can be found in subsection V-I.

G. Propellant Budget

The Propellant Budget is included in Table V. This budget is composed of the Propellant required for the main burns and the attitude control system.

TABLE IV: Margins

Application Area	Factor
System mass	1.2
Propellant mass	1.15
Ullage volume	1.02
Helium tank pressure	1.3
Helium volume/mass	1.2
Helium tank mass	2.5
Propellant tank mass	1.75

TABLE V: Final masses [kg]

Science Instruments (INS)	50
AOGNC	40
Communication (COM)	25
Thermal Control (TC)	15
Deployable Surface Probe	20
Data Handling (DH)	15
Mechanisms (MEC)	55
Propulsion (PROP)	205.01
Power (PWR)	84.358
Structure (STR)	66.967
Harness	64.036
Dry Mass	640.36
System Margin	1.2
Dry Mass incl. System Margin	768.43
Propellant Mass	1328.5
Hydrazine Mass	577.61
NTO Mass	750.89
Helium Mass	4.3094
Total Wet Mass	2097.0

H. Pressure and temperature evolution in pressurization tank and propellant tanks

This section serves to present the results of the temperature and pressure evolution of the helium in both the pressurization tank itself as well as its behavior within the propellant tanks. Important to note here is that due to the large time in between each burn, the temperature of the helium is assumed to reset from maneuver to maneuver, both within the pressurization tank as well as within the propellant tanks. In the helium tank, this also results in a partial pressure reset (i.e. increase) during that time. In the propellant tanks, this differs a little from maneuver to maneuver. Generally, the helium arrives at the respective propellant tank with a temperature lower than the one of the propellants itself. With now assumed mixing of the helium that has already been in the tank from previous maneuvers with the newly arriving helium, average temperatures for

TABLE VI: Final sizes

Tank	Volume [L]	Diameter [m]
Hydrazine	506.82	0.9892
NTO	458.93	0.9570
Helium	98.318	0.5726

TABLE VII: Electrical Power Consumption

Component	Power [W]
Valve, main engine	45
Attitude control system	20
All other subsystems	550
Total	615

said gas can be estimated (taking into account the respective volumes). Between maneuvers and with the helium assuming the temperature of the propellants, a resultant pressure rise can also be estimated using a similar logic. As can also be seen in the graph, it is assumed that during the maneuvers the pressure is regulated so that any excess pressure will vanish during the burns and therefore before rising again due to the reheating, the pressure after each maneuver will be the nominal tank pressure of 15 bars again. The only exception to the just described behavior is during and after the first burn: Since the helium heats up at the regulating valve because of the Joules-Thomson-Coefficient, its temperature after the first burn and when arriving in the propellant tanks is above the propellants storage temperature (for all following maneuvers, this effect is not great enough anymore to compensate for the already cooled helium coming from the pressurization tanks). Therefore, reverse effects come into play for this first burn and the pressure in the propellant tanks indeed drops a little. Theoretically, this might be an issue with regard to supplying the engine with sufficiently pressurized propellants. But since the minimal pressure is still well within the operational chamber pressure of the engine [11], even when considering possible losses as mentioned before, this will not affect the performance. Since both propellants are stored at the same temperature and since no additional complex thermodynamic interactions between the helium gas and the fuel or oxidizer are taken into account, the resulting behavior of the helium in the respective propellant tanks differs only very slightly due to the relatively small difference in mass flow out of the respective tank. To not unnecessarily present (almost) duplicates of the respective graphs, only one is shown each for the temperature and for the pressure evolution, but the behavior holds true for both the hydrazine tank as well as the NTO tank. One last thing to mention here is that the time in-between maneuvers is not plotted, making it appear as if the respective values would jump from one state to another. Naturally, this is not the case and this rather happens over some time (exact timings are not of interest here). However, this is not shown to put the focus on the parts of interest and thereby increase the expressiveness of the charts. The results can be found below, with Figure 5 and Figure 6 showing the temperature and pressure depletion in the helium tank, and Figures Figure 7 and Figure 8 depicting the behavior in the propellant tanks. It is important to note here that while the behavior in the gas tank itself is visualised with accurate timing (apart from the times between the respective burns), the temperature and pressure evolution in the propellant tanks are not precisely calculated with respect to time (while temperature and pressure of the helium flowing in are being computed with exact timing - but not of interest in itself - no assumptions were made for the mixing speed of "new" with "old" helium). For visualization purposes, the temperature adjustment was imagined to happen exactly within the burning time of each maneuver (and then the reset in-between these happens instantly), while the pressure curve was plotted without any specific timings and is meant to represent the behavior after each maneuver.

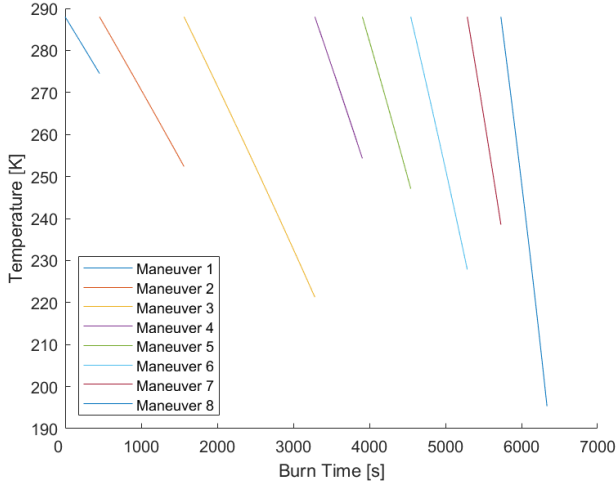


Fig. 5: Temperature evolution, helium tank

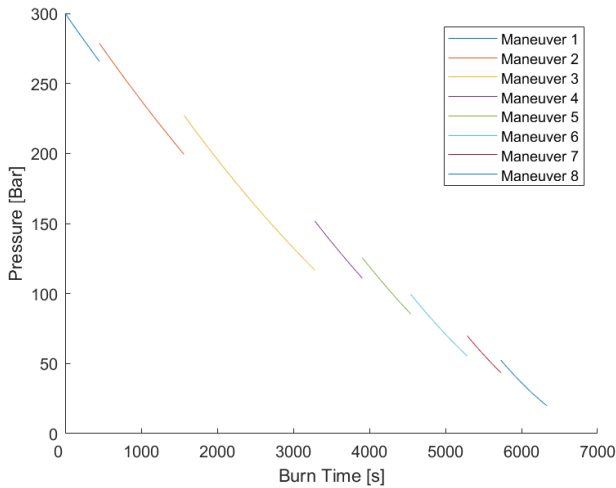


Fig. 6: Pressure evolution, helium tank

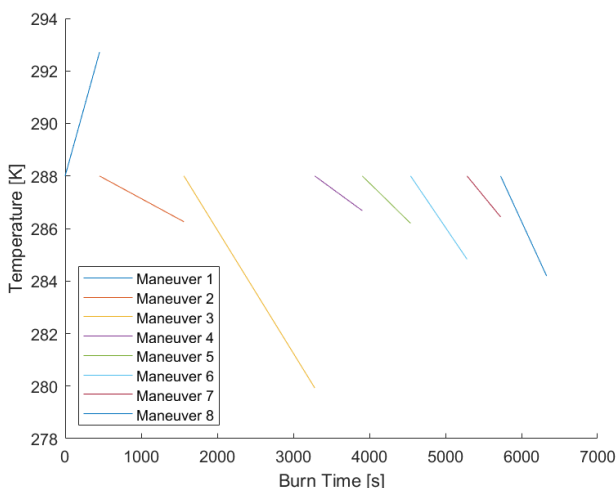


Fig. 7: Helium temperature evolution, propellant tanks

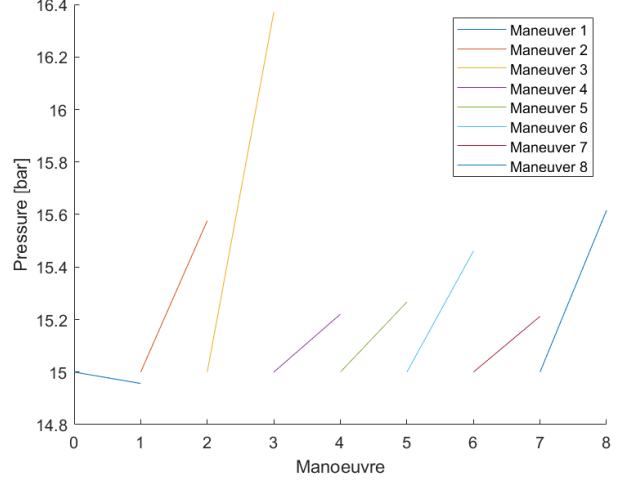


Fig. 8: Helium pressure evolution, propellant tanks

I. Technology Needs

1) *ACS Reaction Wheels:* To calculate each reaction wheel's characteristics, the perturbations encountered throughout the mission are quantified. The most relevant corrections are those related to thrust misalignments and nozzle direction deviations. However, other perturbation effects encountered in space are - solar radiation pressure, Sun third-body problem, and magnetic field disturbances. From these, moments of inertia and dimensions of reaction wheels are calculated from the spacecraft's characteristics. Finally, the minimum angular momentum each reaction wheel must have is calculated. A final value of 27Nm s is obtained. The best commercially available reaction wheel with the corresponding characteristics calculated is the *Rockwell Collins RSI 30-280-30* reaction wheel Figure 9 [35].

The following table includes the main technical data of each reaction wheel.

TABLE VIII: Reaction wheel characteristics

Main Technical Data - RSI 30-280-30	Values
Angular Momentum @ Nominal Speed	30Nm s
Operational Speed Range	3000rpm
Motor Torque @ Nominal Speed	280mNm
Diameter	347mm
Height	124mm
Mass	8.5kg
Power Consumption @ Steady State	20W
Power Consumption @ Maximum Torque	150W

The selected attitude control system (ACS) configuration consists of four reaction wheels and four small thrusters. Three of the reaction wheels are placed in the three major axes of the spacecraft and a fourth reaction wheel is placed in a direction with a vectorial component corresponding to each major axes. This acts as an inhibit in case of a major axes reaction wheel failure, mitigating the probability of

mission failure. An example of the implementation of the four reaction wheels is found in Figure 10.



Fig. 9: Rockwell Collins RSI 30-280-30 reaction wheel.

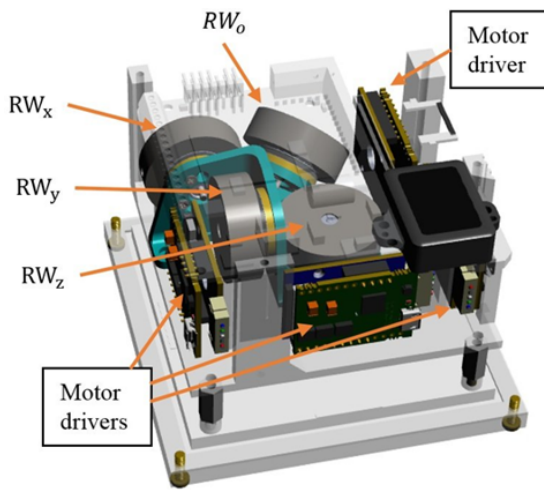


Fig. 10: Example of implementation of four reaction wheels.

2) *ACS Thrusters*: Reaction wheels saturate after achieving nominal speed. Four small thrusters corresponding to each wheel are included as part of the attitude control system and will desaturate their corresponding reaction wheel. To select the best commercial option, the nominal thrust required to desaturate each reaction wheel has been calculated to be 20.9N. Therefore, the best commercial thruster corresponding to the calculated nominal thrust is the *Aerojet Rocketdyne R-6F 22N* thruster [36]. The thruster's schematic is included in Figure 11.

The following table includes the main technical data of each ACS thruster.

The thruster is currently ready for flight qualification and is yet to be produced. However, taking into account that the flight qualification process takes roughly two years [37] and the mission is being launched in 2026, it is expected to be ready previous to the launch date.

TABLE IX: ACS Thruster characteristics.

Main Technical Data - Aerojet Rocketdyne R-6F 22N	Values
Propellant	Hydrazine/NTO
Nominal Thrust	22N
Nominal Specific Impulse	295s
Inlet Nominal Pressure	6.9 – 20.79bar
Valve Power	11W
Mass	0.965kg
Propellant Mass	47.13kg

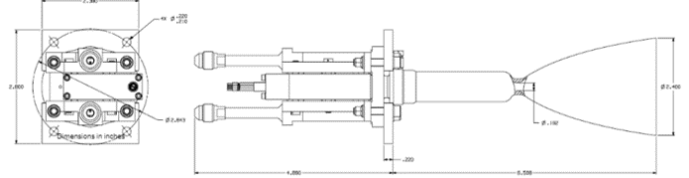
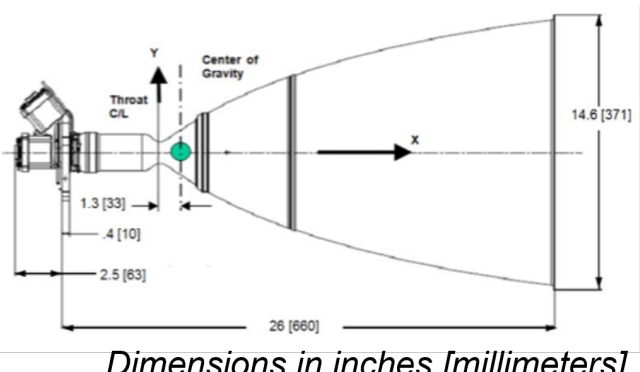


Fig. 11: Aerojet Rocketdyne R-6F 22N attitude control system thrusters.

3) *Main Thruster*: Basing the decision on the trade-off analysis performed in subsection V-B, the selected main engine corresponds to the *Aerojet Rocketdyne AMBR 556N* commercial engine [36]. The thruster's schematic is included in Figure 12. The following table includes the main technical data of the engine.

TABLE X: Main Engine characteristics.

Main Technical Data - Aerojet Rocketdyne AMBR 556N	Values
Propellant	Hydrazine/NTO
Nominal Thrust	556N
Nominal Specific Impulse	329s
Inlet Nominal Pressure	> 14bar
Chamber Pressure	10.3 – 11.7bar
Nominal Mixture Ratio (O/F)	1.0 – 1.3
Demonstrated Steady State Firing Duration	2700s
Valve Power	45W
Mass	4.9kg
Propellant Mass	1338.6kg



Dimensions in inches [millimeters].

Fig. 12: Aerojet Rocketdyne AMBR 556N main engine.

The thruster is currently ready for flight qualification and is yet to be produced. However, taking into account that the flight qualification process takes roughly two years [37] and the mission is being launched in 2026, it is expected to be ready previous to the launch date.

ready previous to the launch date.

4) Tanks: According to the mission sequence and the ΔV requirements, all the commercial tank's minimum volumes correspond to the volumes that are compiled in Table VI. Therefore, suppliers have been listed, and the best options that adapt to the requirements are chosen. Two suppliers are chosen - one for the propellant tanks and one for the pressurant tank. *IHI Aerospace* will provide the propellant tanks [38], while *MT Aerospace* will provide the pressurant tanks [39].

The following two tables correspond to the main technical data provided by the suppliers.

TABLE XI: Propellant tank characteristics.

Main Technical Data - 552L IHI Aerospace Tank	Values
Material	Ti (forging)
Total Volume (unpressurized)	552L
Internal Device	Diaphragm
Size	1087 ID Sphere

TABLE XII: Pressurant tank characteristics.

Main Technical Data - PVG Family 80-120 HPV Tank	Values
Fluids	He, N
Shell Material	Ti-6Al-4V
Tube Material	Ti-3Al-2.5V
Overwrap Material	Epoxy-based CFRP
Total Volume (unpressurized)	80 – 120L
Tank Dry Mass	23.5kg
Diameter (max pressurized)	432.0mm



Fig. 13: Analogue IHI propellant tank.



Fig. 14: MT Aerospace PVG Family 80-120 HPV pressurant tank .

Both tanks are currently in production and show no sign of being discontinued in the short term before the mission departure.

VI. CONCLUSIONS AND FUTURE DIRECTIONS

Project management and regular meetings have had an incredible impact on the development of the spacecraft proposal. Weekly meetings have been held in order to track, validate, and re-discuss potential setbacks through the project's evolution. Interconnectivity between mission design considerations and the spacecraft subsystems has made coordination between team members crucial, proving communication a significant role. Targets and deadlines have become our best allies.

Dimension constraints imposed by Ariane 62 have been met by the spacecraft. All design decisions revolve around optimizing the spacecraft's performance. However, the use of a liquid bi-propellant propulsion system compromises the architecture's Isp for a significantly shorter mission duration, with the intent of limiting the electrical equipment to harmful space radiation. Simultaneously, the ΔV budget has been reduced through planning an adequate mission sequence in GMAT and the consequent impulse burns planned. Critical mission failure has been mitigated through the use of three inhibits and can be contemplated in Figure 4. Additionally, all the Design Challenge requirements have been met (*PROP-010 - PROP-060*), along with several ECSS standards (*ECSS-E-ST-35C Rev. 1*, *ECSS-E-ST-35-01C*).

In future advancements of the project, it is necessary to calculate the overall costs of the spacecraft. This has proven a challenge due to opaque pricing by suppliers and limited resource availability. Validation of the design concept could be addressed through the use of further ECSS standards. Furthermore, by testing the spacecraft, insightful practical data may be collected to help develop the project. Finally, using a different deorbiting strategy - such as aero-assistance - may result beneficial by reducing the ΔV requirements as well as optimizing the corrective maneuvers by implementing new parameters, such as the spacecraft altitude, inclination, and eccentricity.

VII. TEAM SETUP

As stated in section VI, project management was crucial for achieving the results presented in this document. In the beginning, topics were equally rotated among the members of the team to achieve a solid common ground of knowledge and understanding of the process and thus, divided into focused topics at a later stage with constant peer-to-peer review and participation from all the rest of the team members. Research, scripts, and additional material included or used to design the spacecraft's propulsion system have been developed thanks to the coordinated participation of all members.

Angel Sosa has been responsible for the research, assumptions, developing the trajectory, and mission sequence, as well as calculation and adjustment of the ΔV budget to meet the spacecraft requirements. *Anibal Guerrero* has been responsible for developing the P&ID of the propulsion system, the compilation of all subcomponent and commercial ACS thrusters, tanks, and reaction wheel data, developing the technology needs for the propulsion system, and researching future directions. *Christian Racke* has been responsible for the main MATLAB script, total mass and propellant budget, tank sizing, and electrical budget. *Ignacio Zúñiga* has been responsible for the main trade-off analysis, general architecture design, main engine selection, and developing the P&ID. Although team members developed areas of expertise, there was active participation in other tasks besides the main one. Distribution of the workload, tasks, and goals can be seen in Figure 15.

VIII. INDIVIDUAL PART

In this individual report, I will discuss all my contributions to the spacecraft proposal developed. My contributions to the project have proven as vital as the rest towards obtaining an adequate concept design. Furthermore, when deciding upon how I would distribute the work, each team member has always attempted to participate in what they do best or is the most eager to learn. This approach maximized the outcome and helped us move forward more confidently at times in which uncertainty predominated.

Dynamic workloads, management, and interdisciplinary assignments would best describe my role. Initially, without knowing my team members and what they did best, I decided to learn more about them and assess how we could benefit from each other. Then, I proposed to use Miro as an interactive platform in which results could be displayed and Figure 15 was developed. It would track progress, deadlines, and important findings discussed in our weekly meetings, along an hour log so no one was left behind. Once finished with all the administrative talk, the technical information is presented.

First and after my colleagues had finished performing the trade-off analyses, I had the chance to develop the propulsion system architecture from subsection V-C and the corresponding P&ID presented in subsection V-D. The

proposed liquid bi-propellant propulsion system uses Helium as pressurant gas to feed the two tanks of hydrazine and NTO, respectively. The system has a two-tank cylindrical configuration, which has been chosen over a four-tank design because it has fewer valves and pipes, reducing the complexity and increasing the reliability of the mission. The main center of gravity shift is on the z-axis of the satellite, which helps reduce the complexity of the attitude control system, orientate correctly the spacecraft, and ease spacecraft operations.

For the attitude control system, I have chosen a 3-axis stabilized system that includes four reaction wheels, one for each axis, and a redundant one. Additionally, there are four small bi-propellant thrusters for the desaturation of each reaction wheel and for emergency purposes.

Then, I illustrated the system's schematic P&ID in Figure 4. The engine system has been divided into two main sections - the pressurant gas feed system and the propellant feed system. I discussed the pressurant gas tanks in subsubsection V-I4. I selected fill and drain valves to control the flow of fluids in the system by loading or venting the pressurant, and propellants. These valves can be found all throughout the schematic, between every and each closed section. Then, I described the use of pyrotechnic valves that can be found in two states - normally closed and normally opened. The filter's purpose is to protect sensitive components of the architecture, such as pressure regulators, check valves, and thrusters. I then included double-pressure regulators to lower the high He pressures in two stages and to provide a constant delivery pressure without the need for periodic readjustment. After, I used pressure sensors to translate the physical pressure exerted on the sensor as an output signal that can be used with a pressure regulator to control the pressure delivered. Then, I discussed the propellant tanks in subsubsection V-I4 too. The purpose of latch valves is to control the flow of the fluid with precision, as they have low power consumption.

Afterward, I included a more precise explanation of how the mass flow moves around the propulsion system, from the He pressurant tanks, into the propellant tanks, and into the thrusters. It is important to note that a detailed explanation of how critical failure probability has been mitigated through the use of three inhibits. Additional redundancies have also been included. For example, the use of two pressure regulators in parallel and two check valves in series, are in place to secure the correct working of the system in case one fails. Additionally, pressure relief valves are placed to prevent outbursts due to extremely high-pressure irregularities. Further details are discussed in subsection V-D. It is important worth noting that this section has had a contribution effort by *Ignacio Zúñiga*.

As a bonus to the P&ID, a list of all the relevant subcomponents used in the P&ID is included in Table III as

part of subsection V-E. All information has been collected from the suppliers' databases and websites. Within the relevant information lies the unit mass of each subcomponent. These, with the total quantity of each subcomponent used, provides the total masses that have been included as part of the mass budget in Table V in subsection V-G

Then, I calculated the characteristics of the reaction wheels needed for the spacecraft. To do so, I developed a collection of MATLAB scripts used to calculate the effect of the perturbations on the spacecraft. These are attached with the digital appendix. These characteristics are calculated using the perturbations encountered during the mission, such as thrust misalignments, nozzle direction deviations, solar radiation pressure, Sun third-body problem, and magnetic field disturbances. Once I quantified the perturbations, the moments of inertia and dimensions of the reaction wheels are calculated from the spacecraft's characteristics. I then calculated the minimum angular momentum required for each reaction wheel. Then, I chose the best commercial reaction wheel that meets the required characteristics. This was the Rockwell Collins RSI 30-280-30 reaction wheel. The report also includes a table with the main technical data of the reaction wheel all in subsection V-I.

The rest of the technological needs are included in subsection V-I. In this section, I included all the commercial engines, reaction wheels, and tanks selected for the spacecraft, an exhaustive detailing of each has been included in the general report.

Finally, the following Table XIII may be interesting as a quick guide towards finding all relevant information listed previously in this individual report.

Contribution	Reference
Project Management	Figure 15
Propulsion System Architecture	subsection V-C
P&ID Subcomponents	Table III
P&ID Schematic	subsection V-D
Technology Needs	subsection V-I

TABLE XIII: Table with contributions and references found throughout the general report.

This project has proven challenging and enjoyable in equal parts and I am grateful to have been a part of it. It consolidated and expanded prior knowledge, and provided a deeper perspective as to how complex a spacecraft's propulsion system is to develop. Thank you for the opportunity!

REFERENCES

- [1] US Government. *General Mission Analysis Tool (GMAT)*. <https://gmatcentral.org/>. Accessed: March 28, 2023. 2021.
- [2] NASA Jet Propulsion Laboratory. *Interplanetary Mission Design Handbook: Earth-to-Mars Mission Opportunities 2026 to 2045*. JPL Publication 18-11. Pasadena, CA: National Aeronautics and Space Administration, 2018. ISBN: 978-0-9970732-8-1.
- [3] GMAT. *General Mission Analysis Tool (GMAT)*. <https://gmat.sourceforge.net/docs/R2013a/html/SpacecraftOrbitState.html>. Accessed: December 28, 2022. 2021.
- [4] Prof. Dr.-Ing. Chiara Manfletti. *Space Propulsion 1 - Raumfahrtantriebe 1*. Chair if Space Propulsion, TUM School of Engineering and Design, Technical University of Munich, Munich, Germany.
- [5] Martin J. L. Turner. *Rocket and spacecraft propulsion: Principles, practice and new developments*. 3. ed. Springer-Praxis books in astronautical engineering. Berlin: Springer, 2009. ISBN: 978-3-540-69202-7.
- [6] Prof. Dr.-Ing. Chiara Manfletti. *Space Propulsion and Design Challenge*. Chair if Space Propulsion, TUM School of Engineering and Design, Technical University of Munich, Munich, Germany, Winter term 2022.
- [7] Yunus A. Çengel and Michael A. Boles. *Thermodynamics: An engineering approach*. 4. ed. McGraw-Hill series in mechanical engineering. Boston: McGraw-Hill, 2002. ISBN: 0072383321.
- [8] ECSS-E-ST-35-01C - *Liquid and electric propulsion for spacecraft*. Standard. Noordwijk, The Netherlands: ESA-ESTEC Requirements & Standards Division, Nov. 2008.
- [9] ECSS-E-ST-35C – *Propulsion general requirements*. Standard. Noordwijk, The Netherlands: ESA-ESTEC Requirements & Standards Division, 2009.
- [10] ESA. *Technology Readiness Levels Handbook for Space Applications*. Tech. rep. ESA, 2008.
- [11] Aerojet Rocketdyne. *In-Space Propulsion Data Sheets*. Aerojet Rocketdyne, In-Space Propulsion Redmond, Washington, USA, 2019.
- [12] *Spacecraft propulsion, with thrust and precision to the space*. Robert-Koch-Srasse, 182024, Taufkirchen, Germany, 2019.
- [13] Ariane Space. *Chemical bi-propellant thruster family*. Robert-Koch-Srasse, 182024, Taufkirchen, Germany, 2020.
- [14] NASA. *State-of-the-Art of Small Spacecraft Technology, Chapter 4, In-Space Propulsion*. <https://www.nasa.gov/smallsat-institute/sst-soa/in-space-propulsion>. Accessed: March 28, 2023. 2023.
- [15] Aerojet Rocketdyne. *Nuclear Propulsion*. <https://www.rocket.com/space/nuclear-propulsion>. Accessed: March 28, 2023. 2023.
- [16] Yen J. Lii et al. “The DEIMOS Mission: A Low-Cost SmallSat for Multi-Point In Situ Measurements of the Martian Atmosphere and Ionosphere”. In: *Space Science Reviews* 217.1 (2021), p. 12.
- [17] CNES. “The Guiana Space Centre, Europe’s Spaceport: a key site for the development of European space programmes”. In: CNES (2021). URL: <https://cnes.fr/en/guiana-space-centre-europe-spaceport-key-site-development-european-space-programmes>.
- [18] Rod Pyle. *Mission to Mars: an insider’s look at the past, present and future of the red planet*. Prometheus Books, 2015.
- [19] ESA. “ESA’s Deep Space Network: past, present and future”. In: *ESA* (2020). URL: https://www.esa.int/About_Us/ESTEC/ESA_s_Deep_Space_Network_past_present_and_future.
- [20] Mark D. Schaffer, M. Scott Campbell, and Frank M. Long. “Mars B-Plane Analysis for Aerocapture and Precision Landing Missions”. In: *Journal of Spacecraft and Rockets* 41.3 (2004), pp. 361–369.
- [21] Nammo. *Nammo website*. <https://www.nammo.com/product/leros-1c/>. Accessed: March 28, 2023. 2021.
- [22] IHI Aerospace. *Bipropellant Thrusters Lineup*. 900 Fujiki, Tomioka-shi, Gunma-ken 370-2398 Japan, 2019.
- [23] U.S.A DEFENSE LOGISTICS AGENCY. *Standard Prices for Aerospace Energy Category Items*. <https://www.dla.mil/Energy/Business/Standard-Prices/>. 8725 JOHN J. KINGMAN ROAD FORT BELVOIR, VIRGINIA 22060-6222, 2023.
- [24] Ariane Bi-propellants propulsion system scheme. <https://www.space-propulsion.com/>. 2023.
- [25] Rolando Cortes-Martinez and Hugo Rodriguez. “A Total Energy Attitude Control System Strategy for Rigid Spacecraft”. In: *IEEE Access PP* (2019), pp. 1–1. DOI: 10.1109/ACCESS.2019.2934424.
- [26] VACCO. *High Pressure Latch Valves*. https://www.vacco.com/images/uploads/pdfs/latch_valves_high_pressure.pdf. 2019.
- [27] Armin Herbertz. *Spacecraft chemical Propulsion Subsystem Design*. European Space Agency ESA Headquarters 8-10 rue Mario Nikis Paris 75738, France.
- [28] European Space Agency. *Margin philosophy for science assessment studies*. European Space Research and Technology Centre, Keplerlaan 1, 2201 AZ Noordwijk, The Netherlands, 2012.
- [29] MT Aerospace AG. *Spacecraft Propellant Tanks*. MT Aerospace AG, Franz-Josef-Strauss-Strasse 5, 86153 Augsburg, Germany.
- [30] Yiming Zhang, Julian R. G. Evans, and Shoufeng Yang. “Corrected Values for Boiling Points and Enthalpies of Vaporization of Elements in Handbooks”. In: *Journal of Chemical & Engineering Data* 56.2 (2011), pp. 328–337. ISSN: 0021-9568. DOI: 10.1021/je1011086.
- [31] Robert D. McCarty, Hans-Ulrich Steurer, and C.M. Daily. *The thermodynamic properties of nitrogen tetroxide*. Thermophysics Division Center for Chemical En-

-
- gineering, National Engineering Laboratory, National Bureau of Standards, Boulder, Colorado 80303. 1986.
- [32] Terence Tipton et al. “Experimental and theoretical studies of the infrared spectra of hydrazines: N2H4, N2H3D, N2H2D2, N2HD3, and N2D4”. In: *The Journal of Physical Chemistry* 93.8 (1989), pp. 2917–2927. ISSN: 0022-3654. DOI: 10.1021/j100345a015.
- [33] Juan A. McMillan. “Hydrazine-1,1-dimethylhydrazine solid-liquid phase diagram”. In: *Journal of Chemical & Engineering Data* 12.1 (1967), pp. 39–40. ISSN: 0021-9568. DOI: 10.1021/je60032a012.
- [34] Roland Lagier. *Ariane 6 User’s Manual*. ArianeSpace, Boulevard de l’Europe, BP 177 91006 Evry-Courcouronnes Cedex, France, 2021.
- [35] Collins Aerospace. *RSI 30-280-30 Datasheet*. https://satcatalog.s3.amazonaws.com/components/203/SatCatalog_-_Collins_Aerospace_-_RSI_30-280-30_-_Datasheet.pdf?lastmod=20210708033022. 2021.
- [36] *In-Space Propulsion Data Sheets*. <https://docplayer.net/156532169-In-space-propulsion-data-sheets.html>. n.d.
- [37] ESA. *Building and testing spacecraft*. https://www.esa.int/Science_Exploration/Space_Science/Building_and_testing_spacecraft. 2022.
- [38] IHI Corporation. *Tank Lineup*. https://www.ihi.co.jp/ia/en/products/space/tanks/i/Tank_lineup.pdf. n.d.
- [39] MT Aerospace. *Tank Catalog*. <https://www.mt-aerospace.de/files/mta/tankkatalog/MT-Tankkatalog.pdf>. n.d.

APPENDIX

A. Trade-off tables

Appendix A includes all the trade-off analyses performed.

TABLE XIV: Weighting of parameters for the general propellant comparison

	Isp [m/s ²]	Thrust [N]	T mission	Prop. restart	System complexity	Total Mass & Volume	Required Power	Sys. Compatibility	Contamination	Technology Status	Availability	Total Cost
Isp [m/s ²]	X	2	3	1	1	3	2	2	2	3	1	3
Thrust [N]	2	X	3	1	1	3	2	2	2	3	1	3
T mission	1	1	X	1	1	2	1	2	1	2	1	2
Prop. restart	3	3	3	X	2	3	3	2	2	2	1	3
System complexity	3	3	3	2	X	3	2	2	2	3	2	3
Total Mass & Volume	1	1	2	1	1	X	1	1	1	3	1	3
Required Power	2	2	3	1	2	3	X	1	1	3	1	3
Sys. Compatibility	2	2	2	2	2	3	3	X	2	2	1	3
Contamination	2	2	3	2	2	3	3	2	X	2	2	3
Technology Status	1	1	2	2	1	1	1	2	2	X	2	2
Availability	3	3	3	3	2	3	3	3	2	2	X	2
Total Cost	1	1	2	1	1	1	1	1	1	2	2	X
Sum	21	21	29	17	16	28	22	20	18	27	15	30
Weight	0,080	0,080	0,110	0,064	0,061	0,106	0,083	0,076	0,068	0,102	0,057	0,114

TABLE XV: Characteristics comparison of main propellant types

ECSS Criteria	Performance			Mission req.		Resulting Layout			Compatibility and contamination			Experience	Availability of components	
	Sub criteria	Isp [s]	Thrust [N]	T mission	Prop. Re-start	System complexity	Total Mass & Volume	Required Power	Sys. Compatibility	Contamination	Technology Status	Availability	Total Cost	
Hybrid	250	800	Short	Low	Med	High	Low-Med	Med	med	Not flight proved	Low-Med	Med		
Liquid Monopropellant	225	600	Short	Med-High	Med-Low	High	Low-Med	Med	high	Fully developed	High	High		
Liquid Bipropellant	340	1000	Short	Med-High	High	High	Low-Med	Med	high	Fully developed	High	High-med		
Electrostatic	10000	0,5	High	High	Med-high	Low	High	Low	Low-Med	Fully developed	High	Low		
Electromagnetic	5000	200	Med	High	High	Low	High	Low	Low	In Development	Low	Low		
Nuclear (Solid Core)	1000	+1000	Short	Low	Med-high	Med	Med	Low	High	Not flight proved	Low	Low-med		
Other (Solar Sail)	-	~1	High	Low-Med	Low	Low	None	High-Med	low(none)	Flight proved	Low	Low		

TABLE XVI: Trade-off analysis of propellant types

	Isp	Thrust	T. mission	Re-start	Complexity	Mass & Volume	Required Power	Compatibility	Contamination	Tech. Status	Availability	Total Cost	SCORE
Hybrid	2	4	5	2	3	2	4	3	3	3	2	3	3,08
Liquid Monopropellant	2	4	5	4	4	1	4	3	1	5	5	1	3,17
Liquid Bipropellant	2	5	5	4	1	2	4	3	1	5	5	2	3,29
Electrostatic	5	1	1	5	2	5	1	1	4	4	5	5	3,25
Electromagnetic	4	3	3	5	1	5	1	1	5	2	1	5	3,13
Nuclear	3	3	4	1	2	3	2	1	1	3	1	4	2,55
Other(Solar Sail)	2,5	1	1	2	5	4	5	1	5	3	1	5	3,01
Weight	0,080	0,080	0,110	0,064	0,061	0,106	0,083	0,076	0,068	0,102	0,057	0,114	

TABLE XVII: Weighting of parameters for the engine comparison

	Thrust [N]	Isp [s]	Weight [Kg]	TRL	Fuel cost (P+Ox)	Pressure inlet	Contamination	Euro. Supplier
Thrust [N]	X	3	1	2	3	1	1	1
Isp [s]	1	X	1	1	1	1	1	1
Weight [Kg]	3	3	X	2	3	3	2	3
TLR	2	3	2	X	3	3	2	1
Fuel cost (P+Ox)	1	3	1	1	X	1	1	1
Presure inlet	3	3	1	1	3	X	3	3
Contamination	3	3	2	2	3	1	X	3
Euro. Supplier	3	3	1	3	3	1	1	X
Sum	16	21	9	12	19	11	11	13
Weight	0,143	0,188	0,080	0,107	0,170	0,098	0,098	0,116

TABLE XVIII: Comparison of main commercial engines

Thruster	Thrust [N]	Isp [s]	Flow Rate [g/s]	Inlet pressure (bar)	Weight [Kg]	Total Impulse [kN * s]	TRL	Fuel	Oxidizer	Contamination	European supplier	Supplier
400N Apogee Motor	425	321	135	15,0	4,3	-	9	MMH	N2O4, MON-1, MON-3	Moderate	Yes	Ariane
LEROS 1c Apogee Engine	458	324	144,10	17,0	4,76	13200	9	Hydrazine	MON	High	E.E.S	Nammo
LEROS 1b Apogee Engine	635	317	204,20	17,0	4,5	-	9	Hydrazine	MON	High	E.E.S	Nammo
LEROS 4 Interplanetary Engine	1000	321	317,56	15,4	8,41	13600	9	MMH	NTO (MON-3)	Moderate	E.E.S	Nammo
R-4D-11 490 N (110 lbf)	490	317,5	157,32	15,0	3,76	20016	9	MMH	NTO (MON-3)	Moderate	No	Aerojet
R-4D-15 HiPAT™ 445 N (100 lbf) HP	445	322,2	141,31	15,0	5,2	13019	9	MMH	NTO (MON-3)	Moderate	No	Aerojet
R-4D-15 HiPAT™ 445 N (100 lbf) DM HP	445	329	138,30	16,2	5,2	9550	7	Hydrazine	NTO (MON-3)	High	No	Aerojet
R-42DM 890N (200 lbf) DM HP	890	327	277	18,3	7,3	20000	7	Hydrazine	NTO (MON-3)	High	No	Aerojet
AMBR 556 N (125 lbf) DM HP	556	329	172,27	15,0	4,9	5792,9	6	Hydrazine	NTO (MON-3)	High	No	Aerojet
MMH Bipropellant Thrusters	478	316	154,20	17,2	4,53	-	9	MMH	MON-3	Moderate	No	IHI
Hydrazine Bipropellant Thruster	450	329	139,43	16,3	4,14	-	9	Hydrazine	NTO	High	No	IHI

TABLE XIX: Trade-off analysis of commercial engines

Type of head	Thrust [N]	Isp [s]	Weight [Kg]	TRL	Fuel cost (P+Ox)	Presure inlet	Contamination	Euro.	Supplier	SCORE
400N T APOGEE MOTOR	1,0	4,5	9,0	9,0	1,0	7,9	10,0	10,0	10,0	5,75
LEROS 1c Apogee Engine	1,5	6,5	8,1	9,0	10,0	3,6	1,0	5,0	5,0	5,79
LEROS 1b Apogee Engine	4,3	1,7	8,6	9,0	10,0	3,6	1,0	5,0	5,0	5,32
LEROS 4 Interplanetary Engine	10,0	4,5	1,0	9,0	1,0	7,0	10,0	5,0	5,0	5,73
R-4D-11 490 N (110 lbf)	2,0	2,0	10,0	9,0	1,0	10,0	10,0	1,0	1,0	4,69
R-4D-15 HiPAT™ 445 N (100 lbf) HP	1,3	5,3	7,2	9,0	1,0	10,0	10,0	1,0	1,0	4,97
R-4D-15 HiPAT™ 445 N (100 lbf) DM HP	1,3	10,0	7,2	7,0	10,0	5,3	1,0	1,0	1,0	5,83
R-42DM 890N (200 lbf) DM HP	8,3	8,6	3,1	7,0	10,0	1,0	1,0	1,0	1,0	5,81
AMBR 556 N (125 lbf) DM HP	3,1	10,0	7,8	6,0	10,0	7,9	1,0	1,0	1,0	6,26
MMH Bipropellant Thrusters	1,8	1,0	8,5	9,0	1,0	3,2	10,0	1,0	1,0	3,68
Hydrazine Bipropellant Thruster	1,4	10,0	8,6	9,0	10,0	5,1	1,0	1,0	1,0	6,14
Weight	0,143	0,188	0,080	0,107	0,170	0,098	0,098	0,098	0,116	

TABLE XX: Attitude control system comparison

	ISP	Thrust	Complexity	acceleration	Propellant use	satellite type	mass
thruster cold gas	low-mid	high	low	high	Yes	all	1kg + prop
thruster propellant	mid-high	high	med	high	Yes	all	1kg + prop
solar sail	-	low	low	low	No	medium-small	1-50 kg
reaction wheels	-	-	low	low	No	medium-small	1-10 x3
Control moment gyros	-	-	high	better than reaction wheels	No	big (Skylab, ISS)	38kg x 3
Magnetic torques				Limited to eart			
Passive attitude control				Limited to eart			

TABLE XXI: Attitude control system trade-off analysis

	Cost	Complexity	Aceleration	Mass	Score
Thruster cold gas	4	3	4	2	3,083
Thruster propellant	3	2	5	3	3,417
Solar sail	1	5	1	4	2,917
Reaction wheels	4	5	2	5	3,767
Control moment gyros	3	1	3	4	2,150
Weight	0,167	0,167	0,292	0,375	

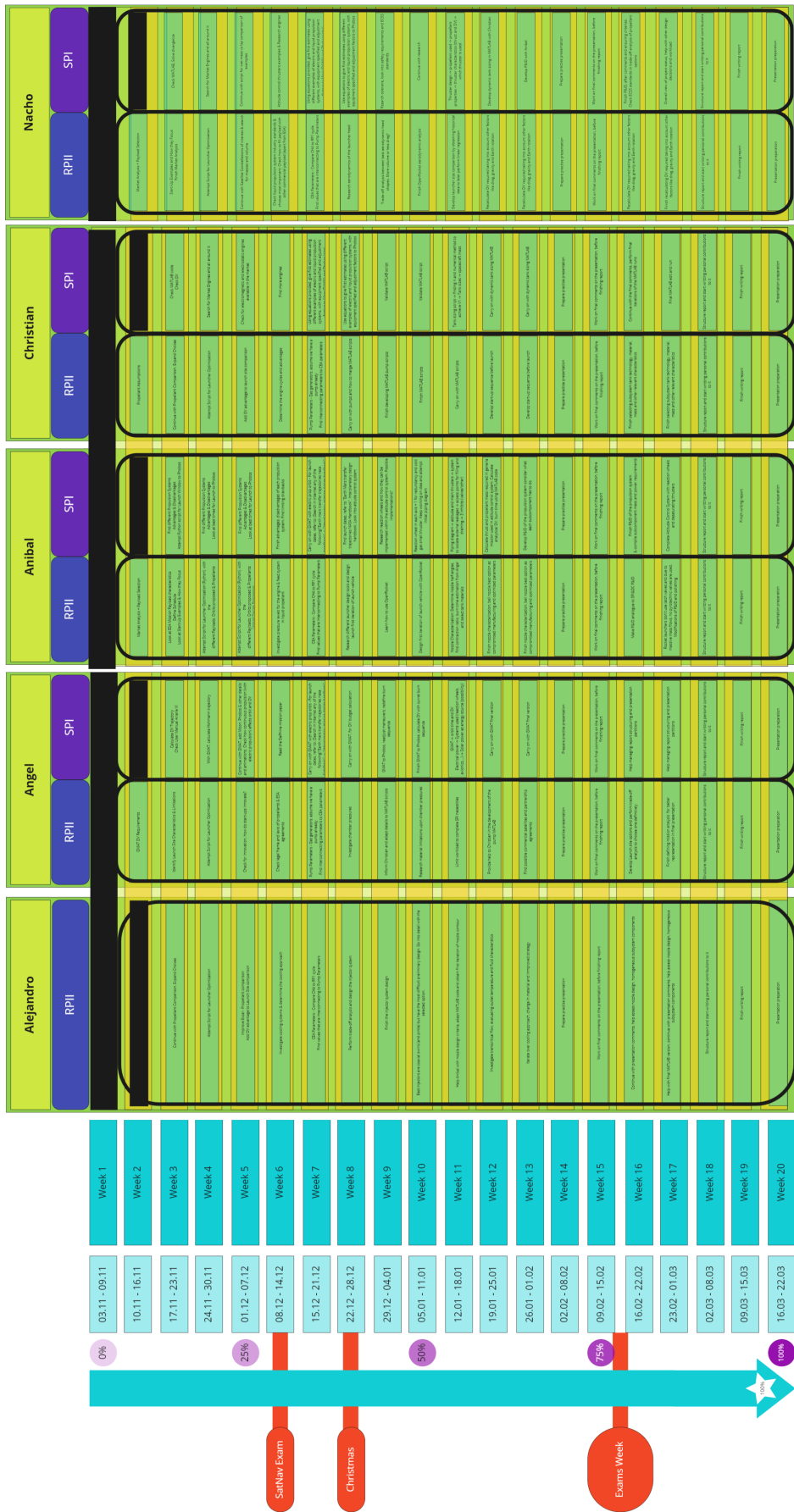


Fig. 15: Task development, work organization, general comments and schedule planned in Miro.

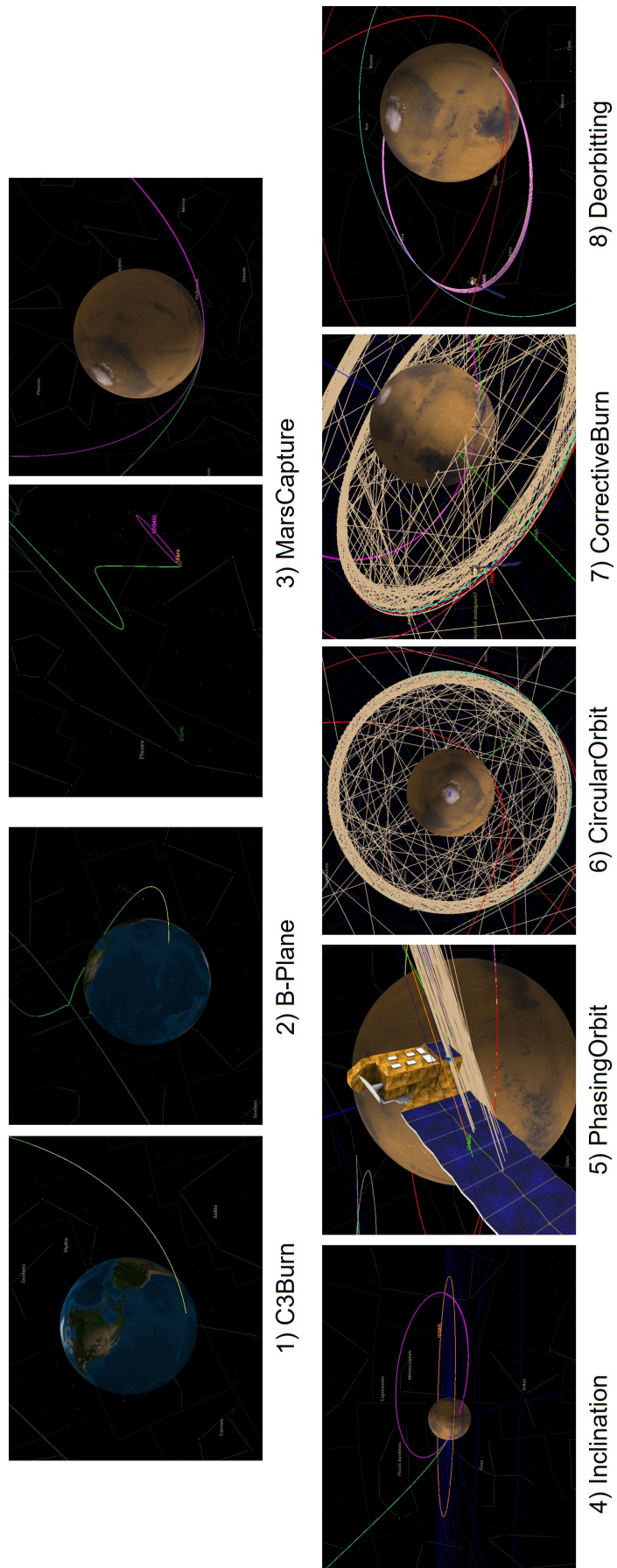


Fig. 16: Visual shoots of GMAT graphics burns from the mission sequence.